Protection of copper against corrosion in neutral solutions by salts of 2-alkylmalonic acids[1]

I.A. Kuznetsov,[1]* A.A. Chirkunov,[1] Yu.I. Kuznetsov,[1] Kh.S. Shikhaliev,[2] M.O. Agafonkina,[1] N.P. Andreeva[1] and Yu.A. Kovygin[2]

[1]A.N. Frumkin Institute of Physical Chemistry and Electrochemistry, Russian Academy of Sciences, Leninsky pr. 31, 119071 Moscow, Russian Federation
[2]Voronezh State University, Universitetskaya pl. 1, 394018 Voronezh, Russian Federation
**E-mail: anarenen@gmail.com*

Abstract

The electrochemical and corrosion behavior of copper in aqueous solutions of sodium salts of alkylmalonic acids with alkyl lengths of $n = 0$, 2, 4, 7 and 9 was studied by ellipsometry, electrochemical impedance spectroscopy (EIS), potentiodynamic polarization and corrosion tests. Addition of alkylmalonic acid salts at a concentration of $C_{inh} = 0.002$ mol/L to borate buffer solution (pH 7.4) containing 0.01 mol/L NaCl slows down the anodic dissolution of copper, increases its local depassivation potential and inhibits the cathodic oxygen reduction. The greater the alkyl length of the inhibitor, the more expressed these effects are. It has been shown that the adsorption strength of alkylmalonate increases with increasing alkyl length and is adequately described by the full Temkin isotherm equation. The standard free energy of adsorption ΔG^0_{ads} of these anions on the oxidized copper surface at $E = 0.0$ V is 47.7 kJ/mol for malonic acid and 83.9 kJ/mol for nonylmalonic acid, which suggests a chemical nature of adsorption. EIS measurements of copper in 0.01 mol/L NaCl solution without and with addition of 0.002 mol/L sodium nonylmalonate showed that after 20 h of tests the protection degree (Z, %) calculated from the values of polarization resistances reaches 99%. Seven-day corrosion tests of copper in 0.01 mol/L NaCl solution performed in the presence of alkylmalonic acid salts with $n = 0$, 2, 4, 7 and 9 have shown that the protective effect increases both with increasing C_{inh} and with increasing alkyl length. In the C_{inh} range of 0.5–3 mmol/L the degree of copper protection by malonic acid anion increases from 26 to 76% and by nonylmalonic acid from 66 to 95% which confirms the highest efficiency of sodium nonylmalonate among the studied dicarboxylates at copper corrosion inhibition.

Received: August 2, 2022. Published: September 21, 2022 doi: 10.17675/2305-6894-2022-11-3-29

[1]This work was carried out with financial support from the Russian Foundation for Basic Research (Grant No. 20-03-00101 “Adsorption of anions of dicarboxylic acids on copper and its alloys and their passivation in neutral solutions”).

Keywords: *corrosion inhibitors, copper, neutral borate buffer, sodium salts of alkylmalonic acids, adsorption, ellipsometry, electrochemical impedance spectroscopy*.

Introduction

Copper and its alloys were used by mankind in ancient times and continue to be widely used at present due to high thermal and electrical conductivity (taking second place after Ag), good mechanical properties and rather easy machinability. In spite of good corrosion resistance in many environments, products made of copper or its alloys corrode when exposed to humid atmosphere or salt solutions, *e.g.* natural or cooling waters. Organic corrosion inhibitors (OCI) [1–4] have long played an important role in protection against corrosion, among which two classes of chemical compounds should be distinguished. One of them includes various azoles, mainly triazoles, whose inhibitory properties, widely discussed in numerous reviews [5–9], are largely related to their ability to form stable complex compounds with Cu(I). Such complexes in many cases form on the surface of metals or alloys insoluble films, preventing its contact with aggressive components of the environment and leading to passivation. The most studied and applied OCI for protection of copper and its alloys in neutral environments is 1,2,3-benzotriazole $C_6H_5N_3$ (BTA), features of protective action of which have been investigated since 1960s [10]. Not surprisingly, by now it is the most studied inhibitor of copper corrosion. The possibility of its adsorption on metal surfaces has been calculated by quantum-chemical methods, which is also confirmed by the results of experiments on copper single crystals [11–14]. Although BTA and other triazoles have a number of advantages, which led to their wide use in neutral and weakly alkaline environments, they are resistant to biodegradation, due to which modern wastewater treatment methods have difficulty removing them. According the data from European chemical agency website (echa.europa.eu), BTA, unlike carboxylic acids and their derivatives, are classified by sanitary and hygienic certificate as chemicals hazardous to the environment.

In this regard, research on their replacement by less toxic and more environmentally friendly OCIs continues [2, 15–20]. Among them a prominent place is occupied by salts of carboxylic acids, described in detail in the monograph [2], and in recent years of great interest are the higher monocarboxylic acids themselves, used to protect copper from corrosion by superhydrophobizing its surface [21–26].

Dicarboxylic acid salts found in some plants or in cell sap can also be non-toxic compounds. In this regard, it can be assumed that when they are used as OCIs, they will not be harmful to the environment. In a review [27] it was noted that the vast majority of studies on carboxylates are devoted to the passivating effect of OCIs against Fe and various steels. It is assumed that the lack of evidence of passivation efficiency of dicarboxylates in relation to steels (compared with monocarboxylates) was one of the reasons for the lack of attention to them from researchers. Thus, the authors [28], comparing the anodic dissolution of mild steel and electrochemical impedance spectroscopy (EIS) data in aqueous solutions of alkyl monocarboxylates (pelargonate, $n = 7$ and caprinate, $n = 8$) and dicarboxylates (azelate and

sebacinate, in which carboxyl groups are separated by alkyl chain with $n = 6$ and 8, respectively) at pH 7.5 found no advantage of dicarboxylates. Analysis of the EIS results allowed us to conclude that the charge transfer resistance value R_p in the monocarboxylate solution is significantly higher than that measured in dicarboxylate solutions, the adsorption of azelate and sebacinate is weak and the layer formed by it has a low diffusion resistance. The reason for this seems to be the observed earlier by K. Aramaki and T. Shimura [29], the adsorption behavior of α,ω-dicarboxylates, in which the interaction with the surface of passive Fe occurs through two carboxyl groups separated from each other. This gives the adsorbed dicarboxylate anion a "loop shape", which prevents the dense packing of the protective film. In this regard, the addition of caprinate to sebacinate improves protection, which creates an opportunity to replace the more toxic BTA in mixtures of it with dicarboxylate.

The protective properties of α,ω-dicarboxylates and alkylcarboxylates in relation to copper in slightly mineralized neutral solutions were first compared back in [30]. It turned out that the R_p value of the copper electrode in α,ω-dicarboxylates solution tends to grow up to $n = 14$ (in contrast to alkylcarboxylates, which sharply decrease the efficiency of copper protection at $n > 10$), although even the most effective in copper protection α,ω-dicarboxylate is slightly inferior to sodium decanoate.

Other effective copper OCIs are the disodium salts of porphyrin derivatives: dimegine [31] and depokolin [32]. Studies of these substances carried out in borate buffer solution containing 0.01 mmol/L NaCl showed that both OCIs passivate copper and effectively prevent its local depassivation by chlorides. The chemisorption of these OCIs on copper due to the oxygen of two carboxyl groups was confirmed by ellipsometry and XPS methods. The strong chemisorption of these dicarboxylates made it possible to use them for surface modification facilitating the subsequent adsorption of another OCI, such as BTA or 5-chloro-BTA.

In recent years, the inhibitory properties against copper corrosion of sodium salts of not only lower (malonic, succinic, ethylmalonic, or adipic acids) [33] but also more hydrophobic alkenylsuccinic acids [34] have been further studied. The spatial proximity of two carboxyl groups in these compounds and the introduction of an alkyl into their molecule, which increases the screening effect and hydrophobicity of the molecule and, consequently, its surface activity, create a prerequisite for creating more effective than α,ω-dicarboxylates inhibitors of copper corrosion. To date, the adsorption and corrosion-preventive properties of alkylmalonates have been studied only for their lower homologues [33], but it is logical to expect that increasing the alkyl length of these compounds can significantly improve their inhibitory properties, for example, with respect to copper.

Experimental

Sodium salts of alkylmalonic acid HOOC–CH(Alk)–COOH with the different number of carbon atoms in the alkyl $n = 2, 4, 7$, and 9 were investigated as adsorbates and OCIs. Malonic and ethylmalonic acids produced by Sigma-Aldrich, CAS numbers 141-82-2 and

601-75-2, respectively. Alkylmalonic acids with $n = 4$, 7, and 9 were synthesized at the Department of Organic Chemistry, Voronezh State University. The parameters of these compounds are presented in Table 1.

Table 1. Parameters of alkylmalonic acids.

Alkylmalonic acid	Molecular weight	Melting point, °C	Purity, % (NMR)
$C_4H_9CH(COOH)_2$	160	102–104	99
$C_7H_{15}CH(COOH)_2$	202	97–98	98
$C_9H_{19}CH(COOH)_2$	230	107–108	98

In the electrochemical and adsorption studies, borate buffer (pH 7.4) was used as the background. It was prepared by mixing solutions in twice distilled water: 0.45 dm^3 0.1 M H_3BO_3 + 0.05 dm^3 0.1 M $Na_2B_4O_7 \cdot 10\ H_2O$ + 1.5 dm^3 water. The studies were carried out on an electrode made of a M1 copper rod (Fe: 0.005%, Ni: 0.002%, S: 0.004%, As: 0.004%, Pb: 0.005%, Zn: 0.004%; the rest is copper) mounted in a Teflon holder so that its working surface was $S = 0.78$ cm^2. It was ground with sandpaper of different grit sizes from P1000 to P2500 and to a mirror shine, and prior to ellipsometric tests it was additionally polished on felt with an aluminum oxide suspension, washed with distilled water, and degreased with acetone. In all the experiments, the electrode potentials E in solutions were measured with respect to the silver chloride reference electrode and their values were converted to the standard hydrogen electrode.

Synthesis of alkylmalonic acids

General methodology for the synthesis of alkylmalonic esters

In an 1 L three-neck flask equipped with stirrer, dropping funnel and reflux condenser with calcium chloride tube, a sodium alcoholate solution is prepared from 1 g-atom of sodium metal and 500 mL of absolute alcohol. To the still hot alcoholate solution, 1 mol of malonic ester and then 1.05 mole of alkyl halide are added dropwise under stirring at such a rate that the reaction mixture slightly boils. Then the mixture is heated under stirring until the sample shows a neutral reaction (2–16 h). The main part of the solvent is distilled off in a weak vacuum under stirring. After cooling down, ice-cold water is added to the precipitate to dissolve the precipitated salt, the organic phase is separated in a separating funnel and the aqueous layer is extracted twice with ether. The combined organic extracts are dried with sodium sulfate, the solvent is distilled off and the residue is fractionated with a 30 cm Vigreux column.

Hydrolysis of alkylmalonic esters

In a 0.5 L flask with reflux condenser 0.5 mol of alkylmalonic ether and 250 mL of 30% sodium hydroxide solution are mixed. The mixture is boiled until homogenization (3–5 h),

then acidified with cold diluted (20%) sulfuric acid to acidic reaction according to the congo. The temperature of the mixture should not rise above +5°C. The precipitated alkylmalonic acid is filtered off, washed with water to neutral pH, and air dried.

Butylmalonic acid: 75% yield, melting point (Mp) 102–104°C. ^{1}H NMR spectrum (DMSO-d_6), (δ, J/Hz): 0.86 (3H, t, J = 6.9, CH_3), 1.20–1.32 (4H, m, $2CH_2$), 1.70 (2H, q, J = 7.6, CH_2), 3.18 (1H, t, J = 7.5, CH), 12.61 (1H, OH). Calculated for $C_7H_{12}O_4$ (160.07): C 52.49%, H 7.55%. Found: C: 52.47%, H 7.57%.

Heptylmalonic acid: 65% yield, Mp 97–98°C. ^{1}H NMR spectrum (DMSO-d_6), (δ, J/Hz): 0.86 (3H, t, J = 6.9, CH_3), 1.17–1.32 (10H, m, $5CH_2$), 1.70 (2H, q, J = 7.6, CH_2), 3.18 (1H, t, J = 7.5, CH), 12.60 (1H, OH). Calculated for $C_{10}H_{18}O_4$ (202.25): C 59.39%, H 8.97%. Found: C 59.20%, H 8.99%.

Nonylmalonic acid: 55% yield, Mp 107–108°C. ^{1}H NMR spectrum (DMSO-d_6), (δ, J/Hz): 0.86 (3H, t, J = 6.9, CH_3), 1.15–1.30 (14H, m, $7CH_2$), 1.69 (2H, q, J = 7.6, CH_2), 3.18 (1H, t, J = 7.5, CH), 12.60 (1H, OH). Calculated for $C_{12}H_{22}O_4$ (230.31): C 62.58%, H 9.63%. Found: C 62.59%, H 9.61%.

Polarization measurements

Electrochemical studies were performed on a copper electrode in a glass cell with separated electrode spaces. Polarization measurements using an IPC-PRO potentiostat (RF) consisted in recording cathodic and anodic polarization curves of copper in a borate buffer solution (pH 7.36) containing 0.01 M NaCl and the studied alkylmalonates.

To improve the reproducibility of polarization curves, a film of air-formed oxide was removed from the copper surface. For this purpose, the electrode was kept for 15 min at the potential E = –0.6 V, then the cell was switched off until free corrosion potential E_{cor} was established, which also took 15 min. After that, the studied OCI was introduced into the solution and after establishing a new value of E_{cor}, the potentiostat was connected and anodic or cathodic polarization was switched on at a 0.2 mV/s potential sweep rate. The potential of local copper depassivation by chlorides (E_{ld}) was determined by a sharp increase in current on the polarization curve followed by visual identification of pitting on the electrode surface. The error in the measurement of E_{ld} is 0.02 V.

Electrochemical impedance spectroscopy (EIS)

The EIS was obtained using an Autolab PGSTAT302 potentiostat with FRA32M module in the frequency f range from 100 kHz to 0.01 Hz with an AC voltage amplitude of 10 mV. The background solution was 0.01 M NaCl solution. The working electrodes were prepared similarly to the electrodes for polarization measurements. The results were processed using the “NOVA” program.

Ellipsometric measurements

The adsorption of alkylmalonate anions on the copper electrode in the present work was studied by ellipsometry, which according to D.E. Aspnes [35] has been one of the main nondestructive methods for determining the surface properties of solids and interfaces since the early 1970s. Its application to study the adsorption of various salts and anions on the surface of such materials as silica [36], calcite [37], and especially various metals [2, 27, 38], including copper, is widely known. A valuable feature of this powerful *in situ* method is the possibility of its application for studying both the formation of ultrathin layers (even smaller than a monolayer) and the properties of polymer films, in particular for the determination of defects in them [39]. The versatility of *in situ* ellipsometry is demonstrated by examples of studied phenomena, such as film expansion, permeation diffusion mechanisms, film degradation, electrochemical processes, *etc*.

Studies of adsorption on the copper surface from neutral borate buffer solution were performed on a Rudolf Research handheld ellipsometer with a $\lambda = 640$ nm HeNe laser, light flux modulation, and a photomultiplier tube as a recorder of light reflected from the surface. During the experiment, ellipsometric angles – phase shift Δ and angle Ψ are determined. A special cylindrical Teflon cell with quartz windows for the entrance and exit of light was used to perform simultaneous electrochemical and ellipsometric measurements.

The electrode, as in the polarization studies, was a copper rod mounted in a Teflon holder. In the solution, the potential on the electrode was maintained using a potentiostat (PAR model 173). The air-formed oxide was removed from the surface by reduction at $E = -0.60$ V for 15 min. When the potential was switched to $E = 0.0$, Cu(I) oxide grew on the copper surface. After 30–40 min the growth of the oxide stops. The thickness of the oxide is equal to ≈1 nm. This surface condition corresponds to Δ_0. An inhibitor concentrate was injected into the cell and the angle Δ was recorded in time. Usually during adsorption the angle Δ increases, *i.e.* $d\Delta = (\Delta - \Delta_0) < 0$. The accuracy in determining Δ was ±0.05°.

From the dependence of $\delta\Delta$ on C_{inh}, we obtained an isotherm of the change in angle Δ. When the angle Δ stops changing when another C_{inh} is added, it was taken as achievement of degree of filling $\Theta \rightarrow 1$. The obtained isotherms of adsorption of these compounds were adequately described by the full Temkin equation, the solution of which is given in [40]:

$$\theta = \frac{1}{f} \ln \frac{1 + n^{-1} B_{max} (C - C_0)}{1 + n^{-1} B_{min} (C - C_0)} \quad (1)$$

where f is the surface energy heterogeneity factor characterizing the change in the enthalpy of adsorption with surface filling, C is the concentration in the solution volume of adsorbing OCI (in units of mol/L); C_0 is the minimum value of OCI concentration from which adsorption effects begin to be recorded, in this case – changes in the ellipsometric angle Δ; n is the molar concentration of water, $n = 55.5$ mol/L. B_{max} and B_{min} are the adsorption

equilibrium constants corresponding to the highest and lowest values of the standard adsorption free energy (ΔG_a^0).

$$B_{\max(\min)} = \exp\left[-\Delta G^0_{a,\max(\min)} / RT\right], \quad (2)$$

where R is the gas constant and T is the absolute temperature. The f, $B_{\max}$ and $B_{\min}$ values are unknown quantities.

The reference electrode was the silver chloride electrode and the auxiliary electrode was the pyrographite electrode. The potentials of electrode E were measured with respect to the silver chloride electrode; in the article, these values are given relative to the standard hydrogen electrode.

Corrosion testing

Corrosion studies were carried out in 0.01 M and 3.5% NaCl solutions in distilled water. Copper plates of dimensions 30×50×3 mm were used as samples for the studies. The samples were cleaned on abrasive paper with grain size from P360 to P1000, degreased with acetone and air dried for 5 min. Then the samples were weighed on electronic scales with an error of measurement of 0.00005 g. The plates were placed in corrosion cells with NaCl solution and with a certain amount of OCI. The cell contained 100 mL of solution, and two samples were placed in each cell so that they did not touch each other and were completely immersed in the solution. The cells were kept in conditions of natural aeration. As the experiment progressed, water was added to the level corresponding to 100 mL of the solution, if necessary. The experiment was performed at room temperature: 22±2°C. After 7 days, the samples were taken out, immersed for 3 s in HCl solution, after that the remaining corrosion products were removed, then samples were dried, and weighed again. From the difference in masses of the samples before and after the experiment, the corrosion rate was calculated for the inhibited solution K_{in} and for the uninhibited K_0 (K [g/m^2·d]. According to the difference in masses, the degree of protection Z was determined by the formula:

$$Z = \frac{K_0 - K_{inh}}{K_0} \cdot 100\% \quad (3)$$

Results and Discussion

Polarization measurements

The introduction of alkylmalonic acid salts in the borate buffer solution with pH 7.4 containing 10 mmol/L NaCl in the concentration C_{inh} = 3 mmol/L equal for all, leads to a slight shift of E_{cor} in the positive direction, most noticeable in the case of C_9 (Figure 1, Table 2). The inhibitory effect in the area of active dissolution is observed for all compounds studied, which is expressed in a decrease in the passivation current density. At the same time, the most hydrophilic C_0 and C_2 weakly interfere with local copper depassivation and an appreciable shift of E_{ld} is observed beginning from C_4. The hydrophobicity of a compound

is characterized by the logarithm of its distribution coefficient in a system of two immiscible liquids, usually octanol and water: log*P* for neutral molecules, log*D* for dissociated molecules. The calculated values of these constants (Table 2) show that the hydrophobicity of alkylmalonate molecules increases naturally with increasing hydrocarbon chain length, although their anions remain hydrophilic. As the hydrophobicity increases, the surface activity of alkylmalonates increases and, consequently, increases their inhibitory effect. A similar pattern is observed on the cathodic polarization curves: the current density decreases as the alkyl length in the OCI molecule increases. The maximum inhibition of partial electrode reactions among the compounds studied is provided by C_9. Figure 2 shows the anodic polarization curves for different concentrations of C_9. Already at $C_{inh} = 0.5$ mmol/L, the decrease of passivation current density is observed by more than an order of magnitude, and at $C_{inh} = 3$ mmol/L the first peak on the anodic curve corresponding to Cu^0/Cu^+ transition is completely suppressed. As the concentration of C_9 additive increases, E_{cor} and E_{ld} also increase.

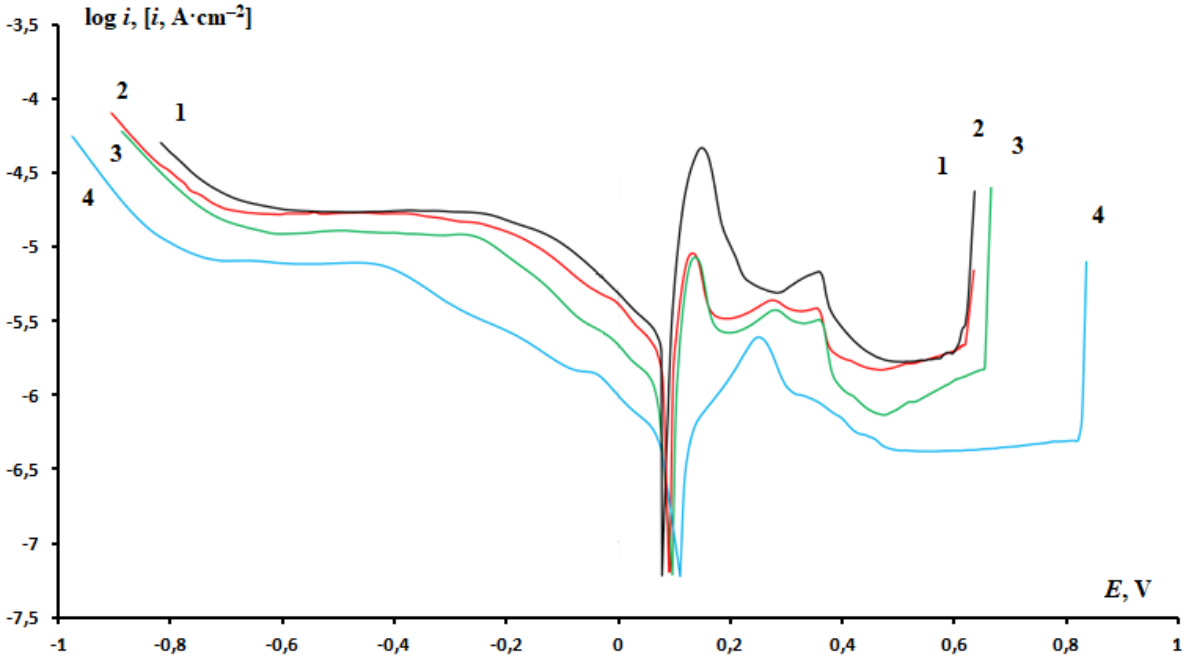

Figure 1. Polarization curves of copper in borate buffer solution pH 7.4 containing 10 mmol chloride without (1) and with the addition of 3 mmol/L OCI: C_0 (2), C_2 (3) and C_9 (4).

Table 2. Comparative characteristics of alkylmalonic acids.

Acid	log*P*	log*D*	E_{cor}, V	E_{ld}, V	$-\Delta G^0_{ads}$, kJ/mol
Background	–	–	0.079	0.62	–
Malonic (C_0)	–0.56	–5.26	0.092	0.63	47.7
Ethylmalonic (C_2)	0.32	–4.38	0.098	0.66	69.4

Acid	log*P*	log*D*	E_{cor}, V	E_{ld}, V	$-\Delta G^0_{ads}$, kJ/mol
Buthylmalonic (C_4)	1.38	–3.27	0.094	0.73	77.7
Heptylmalonic (C_7)	2.98	–1.68	0.095	0.78	78.3
Nonylmalonic (C_9)	4.04	–0.62	0.112	0.82	83.9

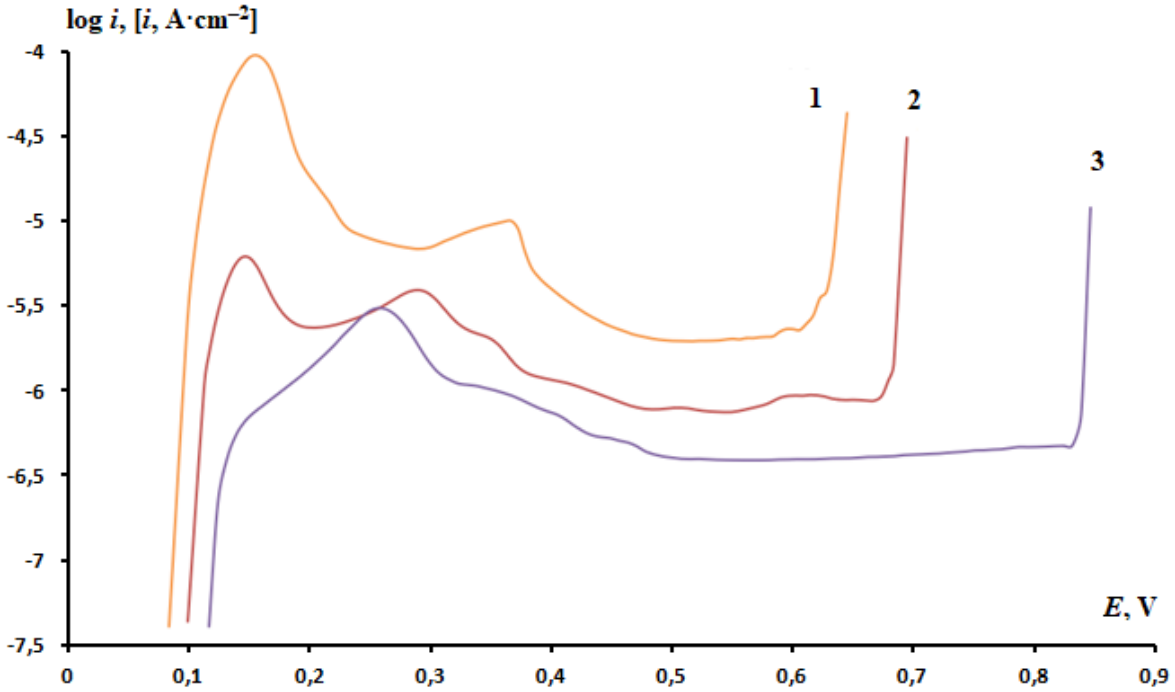

Figure 2. Anodic polarization curves of copper in borate buffer solution pH 7.4 containing 10 mmol/L NaCl (1) and C9 additive: 2 – 0.5 mmol/L, 3 – 3 mmol/L.

Adsorption of alkylmalonic acid anions

The influence of carboxylates on the corrosion resistance of copper is directly related to the adsorption of their anions on the copper surface. The study of the adsorption of OCI in borate buffer with pH 7.4 on the pre-oxidized copper surface at $E = 0.0$ V was carried out *in situ* by ellipsometric method. Adsorption of malonate anions begins at $C_{inh} = 10^{-7}$ mol/L. For anions containing longer alkyls it becomes even lower: a sharp jump by 4 orders of magnitude is observed in the transition from malonate to ethyl malonate, and then it changes not so much, to 2.5 orders of magnitude lower for sodium nonylmalonate. This is due to the increasing hydrophobicity of the corresponding acids.

Building the plot of $(-\delta\Delta)$ *vs.* lg*C* (Figure 3) showed that adsorption of all studied alkylmalonates on copper is adequately described by the full Temkin equation (1), from which we calculated the values $-\Delta G^0_{ads}$, of adsorbate (Table 2), characterizing the bond strength of OCI with the electrode surface. This value is 47.7 kJ/mol for sodium malonate and monotonically increases with increasing number of carbon atoms in hydrocarbon chain

of molecules, reaching a maximum of 83.9 kJ/mol for sodium nonylmalonate. Considering such high values $-\Delta G^0_{ads}$, we can conclude that all the alkylmalonates under these conditions are chemisorbed on the copper electrode.

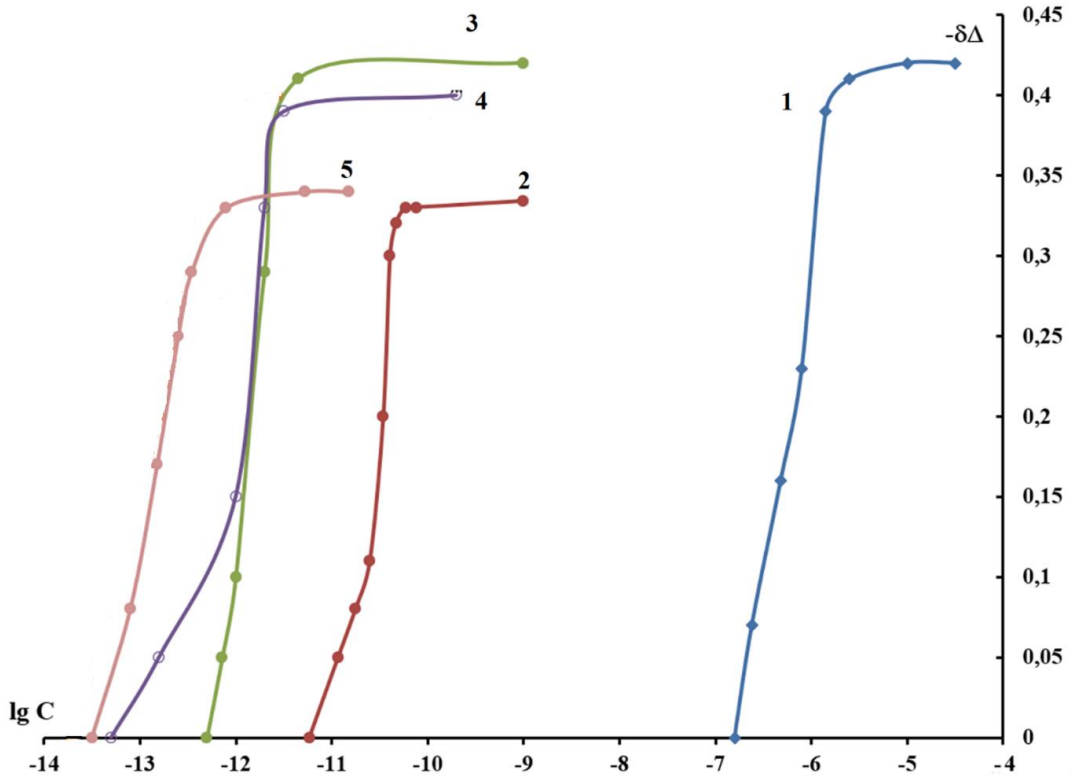

Figure 3. Dependence of change in ellipsometric angle –δΔ on concentration of sodium salts of dicarboxylic acids: 1 – malonic, 2 – ethylmalonic (C_2), 3 – butylmalonic (C_4), 4 – heptylmalonic (C_7), 5 – nonylmalonic (C_9) in borate buffer solution pH 7.4 on an oxidized copper surface at $E = 0.0$ V.

It is interesting to compare these data with the results of adsorption measurements on copper obtained earlier in the same solution of carboxylate OCIs, which can inhibit the corrosion of this metal [42]. Thus, for sodium oleate and sodium oleylsarcosinate, the values $-\Delta G^0_{ads}$, are 39.6 and 54.8 kJ/mol, respectively. Already at alkyl length $n = 2$, *i.e.*, for ethylmalonate, $-\Delta G^0_{ads} = 69.4$ kJ/mol, which exceeds this value for oleylsarcosinate. This can probably be explained by the fact that the studied alkylmalonates, in contrast to oleate and oleilsarcosinate, have two carboxyl groups that directly bind to the electrode surface, which provides a stronger bond of these anions with it.

Electrochemical impedance spectroscopy

Figure 4 shows the Nyquist diagrams for the copper electrode in 0.01 M NaCl solution. The impedance spectra obtained in the absence of OCI are described by the equivalent electrical circuit (EEC) in Figure 5a.

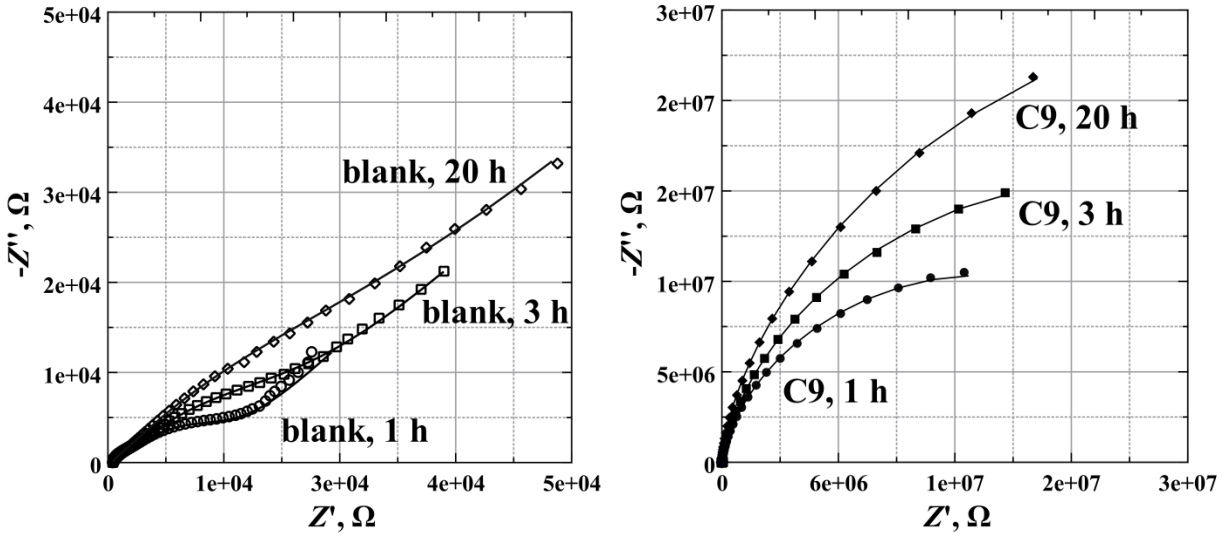

Figure 4. Nyquist diagrams obtained on copper in 0.01 M NaCl in the absence of OCI (background), and in the presence of 2 mM sodium nonylmalonate.

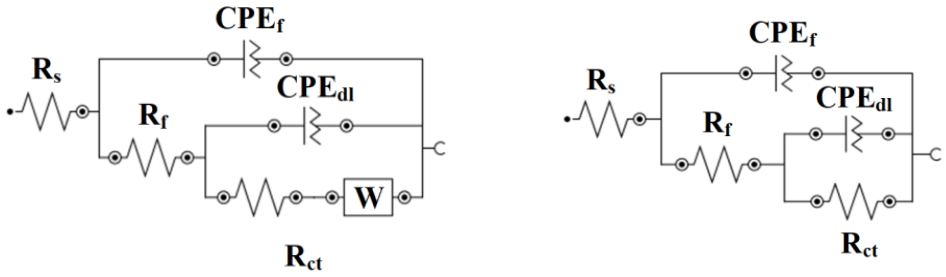

Figure 5. Electrical equivalent circuits used to model EIS data: (a) in a solution without OCI; (b) in a solution containing 2 mM nonylmalonate.

In these schemes R_s represents solution resistance, R_f – surface film resistance, R_{ct} – charge transfer resistance, CPE_f and CPE_{dl} – constant phase elements characterizing the surface film and double electric layer respectively, W – Warburg impedance, characterizing the diffusion layer at the metal–electrolyte interface.

The appearance of Nyquist diagrams changes markedly when passing to the solution containing OCI, and to describe the data obtained in the presence of 2 mM sodium nonylmalonate, the same EEC was used, but without the Warburg impedance (Figure 5b). This is due to the limitation of diffusion of electroactive ions, *i.e.*, Cu^+ or Cu^{2+} in the presence of the OCI film on the copper surface. The capacitive loops are not perfect semicircles due to the inhomogeneity of the electrode surface, so the constant phase element (CPE), which is related to the impedance by the following equation, is used for the calculations:

$$Z_{CPE} = Q^{-1}(i\omega)^{-n} \quad (4)$$

where Q is the ratio, ω is the angular frequency, and n is the exponential exponent denoting the phase deviation, $0 \leq |n| \leq 1$. For integer values of $n = 1$, 0, and –1 the CPE can be simplified

to the classical elements: capacitance (C_{dl}), resistance (R) and inductance (L) respectively, while at $n = 0.5$, CPE gives the Warburg impedance.

The calculated parameters of the EEC elements are presented in Table 3.

Making EIS measurements over time in these solutions and calculating the corresponding EEC elements, we found that in the solution without OCI, the values of R_f and R_{ct} increase with increasing duration of exposure of the copper electrode in it. This indicates the formation of a layer of corrosion products on the electrode surface, which slows down further dissolution of copper.

The Nyquist diagrams obtained in the inhibited solution show a significant increase in the radius of the hodographs and by several orders of magnitude compared to the background solution and increase the values of R_f and R_{ct}. Based on the obtained resistance values we calculated the degree of corrosion protection of copper by OCI (Z%):

$$Z(\%) = [R_p - R_p^0 / R_p] \cdot 100 \quad (6)$$

where $R_p = R_f + R_{ct}$ and represents the polarization resistance, and R_p and R_p^0 refer, respectively, to the inhibited and background solution. The values of R_p and Z, depending on the exposure time of the electrode in the solution, are also presented in Table 3.

Table 3. Values of EEC parameters.

	Without OCI			**2 mmol/L of nonylmalonate**		
τ, h	**1**	**3**	**20**	**1**	**3**	**20**
R_1	501.23	522.97	520.08	470.79	458.29	456.59
CPE_1						
Y_0	2.5835E–06	3.791E–06	1.5983E–05	2.8668E–07	2.8144E–07	2.982E–07
n	0.82078	0.80138	0.65924	0.97864	0.98253	0.98652
R_2	2748.2	2926.1	4171.8	1.2146E+06	2.9514E+06	1.0716E+07
CPE_2						
Y_0	2.32E–05	3.0882E–05	2.7178E–05	1.2457E–07	1.1206E–07	1.0884E–07
n	0.6465	0.60169	0.55423	0.57154	0.59979	0.62012
R_3	11389	23051	49690	3.0579E+07	4.2309E+07	6.005E+07
W	2.3423E–4	1.2963E–4	7.2396E–05	–	–	–
Rp	14137.2	25977.1	53861.8	31793600	45260400	70766000
Z, (%)	–	–	–	99.95	99.94	99.92

Although R_p^0 in the background solution increases over time, the increase in R_p in the presence of sodium nonylmalonate is significantly higher. The calculation shows that the Z value remains almost constant and exceeds 99%. Thus, sodium nonylmalonate provides a

high degree of copper protection, and the increase in R_f and R_{ct} values within 20 h indicates that the formation and perfection of the protective film continues in time.

Corrosion tests

The results of corrosion tests confirm the conclusions that the protective ability of alkylmalonates increases with increasing alkyl length. Thus, at a concentration of 0.5 mmol/L, the protective effect Z was 26% for malonate, increased monotonically with increasing hydrocarbon chain length, and reached a value of 66% for $n = 9$. Nonylmalonate solution with a concentration of 3 mmol/L showed the highest efficiency; in this case, the protective effect was 95%, which agrees with the electrochemical studies. The pH of the solutions was in the region of 6–7.

Table 4. Results of 7-day corrosion tests of copper in 0.01 M NaCl solution and its degree of protection by sodium salts of alkylmalonates.

Concentration, mol·10^{-3}/L	***Z*, %**				
	Malonate	**C_2**	**C_4**	**C_7**	**C_9**
0.5	26	46	55	55	66
1.0	57	68	72	68	86
1.5	65	71	75	70	89
2.0	74	76	–	–	–
3.0	76	77	79	82	95

Conclusions

1. Sodium nonylmalonate inhibits the anodic dissolution of copper better than its lower homologues and stabilizes its passive state by increasing the potential of local depassivation in borate buffer solution with pH 7.4 containing 0.01 mol/L NaCl. It also slows down the cathodic oxygen reduction reaction on copper more strongly, exhibiting pronounced properties of a mixed-type OCI.
2. According to ellipsometric data, the adsorption of sodium alkylmalonates on the oxidized copper surface (at $E = 0.0$ V) is adequately described by the full Temkin isotherm equation. The calculated standard adsorption free energies $-\Delta G^0_{ads}$ increase in the series from malonate (47.7 kJ/mol) to nonylmalonate (83.9 kJ/mol). This increase correlates with an increase in the number of carbon atoms in the alkyl and, consequently, with an increase in the hydrophobicity of the OCI molecules or anions.
3. EIS measurements showed that for the copper electrode in 0.01 mol/L NaCl solution with 2 mmol/L nonylmalonate for 20 h the protective properties of OCI film increase due to its stabilization with time and the protection degree Z exceeds 99%.

4. Seven-day corrosion tests in 0.01 mol/L NaCl solution showed that sodium nonylmalonate has the greatest degree of protection against corrosion of copper among the studied homologues, reaching $Z = 95\%$ at a concentration of 3 mmol/L. At the same time, the protective effect increases both with increasing substance concentration and with the transition from lower homologues to higher ones.

References

1. *Corrosion Inhibitors*, A Working Party Report of European Federation of Corrosion Inhibitors, 1994, London, The Institute of Materials, 163 pp.
2. Yu.I. Kuznetsov, *Organic Inhibitors of Corrosion of Metals*, New York, Plenum Press, 1996, 283 pp.
3. G. Schmitt, Corrosion Inhibitors in the Mirror of the Ferrara Conferences, In Proceedings of 10th European Symposium on Corrosion and Scale Inhibitors, 2005, Ferrara (Italy), University of Ferrara, **2**, 1075–1116.
4. M.B. Petrović Mihajlović and M.M. Antonijević, Copper Corrosion Inhibitors. Period 2008–2014. A Review, *Int. J. Electrochem. Sci*., 2015, **10**, 1027–1053.
5. Yu.I. Kuznetsov and L.P. Kazansky, Physicochemical aspects of metal protection by azoles, *Russ. Chem. Rev*., 2008, **77**, no. 3, 219–232. doi: 10.1070/RC2008v077n03ABEH003753
6. Z. Chen, L. Huang, G. Zhang, Y. Qui and X. Guo, Benzotriazole as a volatile corrosion inhibitor during the early stage of copper corrosion under adsorbed thin electrolyte layers, *Corros. Sci*., 2012, **65**, 214–222. doi: 10.1016/j.corsci.2012.08.019
7. N.K. Allam, A.A. Nazeer and E.A. Ashour, A review of the effects of benzotriazole on the corrosion of copper and copper alloys in clean and polluted environments, *J. Appl. Electrochem*., 2009, **39**, 961–969. doi: 10.1007/s10800-009-9779-4
8. M. Finšgar and I. Milošev, Inhibition of copper corrosion by 1,2,3-benzotriazole: A review, *Corros. Sci*., 2010, **52**, 2737–2749. doi: 10.1016/j.corsci.2010.05.002
9. D. Gopi, K.M. Govindaraju, V. Collins Arun Prakash, D.M. Angeline Sakila and L. Kavitha, A study on new benzotriazole derivatives as inhibitors on copper corrosion in ground water, *Corros. Sci*., 2009, **51**, 2259–2265. doi: 10.1016/j.corsci.2009.06.008
10. I. Dugdale and J.B. Cotton, An electrochemical investigation on the prevention of staining of copper by benzotriazole, *Corros. Sci*., 1963, **3**, 69–74. doi: 10.1016/S0010-938X(63)80001-3
11. N. Kovačević, I. Milošev and A. Kokalj, How relevant is the adsorption bonding of imidazoles and triazoles for their corrosion inhibition of copper?, *Corros. Sci*., 2017, **124**, no. 1, 25–34. doi: 10.1016/j.corsci.2017.04.021
12. F. Grillo, D.W. Tee, S.M. Francis, H.A. Früchtl and N.V. Richardson, Passivation of Copper: Benzotriazole Films on Cu(111), *J. Phys. Chem. C*, 2014, **118**, no. 16, 8667–8675. doi: 10.1021/jp411482e

13. G. Rajkumar and M.G. Sethuraman, Corrosion protection ability of self-assembled monolayer of 3-amino-5-mercapto-1,2,4-triazole on copper electrode, *Thin Solid Films*, 2014, **562**, 32–36. doi: 10.1016/j.tsf.2014.03.074
14. A. Kokalj, *Ab initio* modeling of the bonding of benzotriazole corrosion inhibitor to reduced and oxidized copper surfaces, *Faraday Discuss*., 2015, **180**, 415–438. doi: 10.1039/C4FD00257A
15. B. Lin and Y. Zuo, Corrosion inhibition of carboxylate inhibitors with different alkylene chain lengths on carbon steel in an alkaline solution, *RSC Adv*., 2019, **9**, 7065–7077. doi: 10.1039/c8ra10083g
16. E. Rocca, G. Bertrand, C. Rapin and J.C. Labrune, Inhibition of copper aqueous corrosion by non-toxic linear sodium heptanoate: mechanism and ECAFM study, *J. Electroanal. Chem*., 2001, **503**, 133–140. doi: 10.1016/S0022-0728(01)00384-9
17. E. Abelev, D. Starosvetsky and Y. Ein-Eli, Enhanced Copper Surface Protection in Aqueous Solutions Containing Short-Chain Alkanoic Acid Potassium Salts, *Langmuir*, 2007, **23**, no. 22, 11281–11288. doi: 10.1021/la701434e
18. S. Ramesh and S. Rajeswari, Evaluation of inhibitors and biocide on the corrosion control of copper in neutral aqueous environment, *Corros. Sci*., 2005, **47**, no. 1, 151–169. doi: 10.1016/j.corsci.2004.05.013
19. A. Fateh, M. Aliofkhazraei and A.R. Rezvanian, Review of Corrosive Environments for Copper and its Corrosion Inhibitors, *Arabian J. Chem*., 2017, **13**, no. 1, 481–544. doi: 10.1016/j.arabjc.2017.05.021
20. H. Tian, W. Li, K. Cao and B. Hou, Potent inhibition of copper corrosion in neutral chloride media by novel non-toxic thiadiazole derivatives, *Corros. Sci*., 2013, **73**, 281–291. doi: 10.1016/j.corsci.2013.04.017
21. T. Liu, Y. Yin, S. Chen, X. Chang and S. Cheng, Super-hydrophobic surfaces improve corrosion resistance of copper in seawater, *Electrochim. Acta*, 2007, **52**, 3709–3713. doi: 10.1016/j.electacta.2006.10.059
22. T. Liu, S. Chen, S. Cheng, J. Tian, X. Chang and Y. Yin, Corrosion behavior of super-hydrophobic surface on copper in seawater, *Electrochim. Acta*, 2007, **52**, 8003–8007. doi: 10.1016/j.electacta.2007.06.072
23. P. Wang, R. Qiu, D. Zhang, Z. Lin and B. Hou, Fabricated super-hydrophobic film with potentiostatic electrolysis method on copper for corrosion protection, *Electrochim. Acta*, 2010, **56**, 517–522. doi: 10.1016/j.electacta.2010.09.017
24. Y. Huang, D.K. Sarkar and X.-G. Chen, A one-step process to engineer super-hydrophobic copper surfaces, *Mater. Lett*., 2010, **64**, 2722–2724 doi: 10.1016/j.matlet.2010.09.010
25. Y. Huanga, D.K. Sarkara, D. Gallant and X-G. Chen, Corrosion resistance properties of superhydrophobic copper surfaces fabricated by one-step electrochemical modification process, *Appl. Surf. Sci*., 2013, **282**, 689–694. doi: 10.1016/j.apsusc.2013.06.034

26. P. Wang, D. Zhang and Z. Lu, Advantage of Super-hydrophobic Surface as a Barrier against Atmospheric Corrosion Induced by Salt Deliquescence, *Corros. Sci*., 2015, **90**, 23–32. doi: 10.1016/j.corsci.2014.09.001
27. Yu.I. Kuznetsov, Organic corrosion inhibitors: where are we now? A review. Part II. Passivation and the role of chemical structure of carboxylates, *Int. J. Corros. Scale Inhib*., 2016, **5**, no. 4. 282–318. doi: 10.17675/2305-6894-2016-5-4-1
28. U. Rammelt, S. Köhler and G. Reinhard, Electrochemical characterization of the ability of dicarboxylic acid salts to the corrosion inhibition of mild steel in aqueous solutions, *Corros. Sci*., 2011, **53**, 3515–3520. doi: 10.1016/j.corsci.2011.06.023
29. K. Aramaki and T. Shimura, Self-assembled monolayers of carboxylate ions on passivated iron for preventing passive film breakdown, *Corros. Sci*., 2004, **46**, 313–328. doi: 10.1016/S0010-938X(03)00156-2
30. G.T. Hefter, N.A. North and S.H. Tan, Organic corrosion inhibitors in neutral solutions. Part 1. Inhibition of steel, copper and aluminum by straight chain carboxylates, *Corrosion*, 1997, **53**, 657–667. doi: 10.5006/1.3290298
31. Yu.I. Kuznetsov, M.O. Agafonkina, N.P. Andreeva and L.P. Kazansky, Adsorption of dimegin and inhibition of copper dissolution in aqueous solutions, *Corros. Sci*., 2015, **100**, 535–543. doi: 10.1016/j.corsci.2015.08.028
32. O.Yu. Grafov, L.P. Kazansky, S.V. Dubinskaya and Yu.I. Kuznetsov, Adsorption of depocolin and inhibition of copper dissolution in aqueous solutions, *Int. J. Corros. Scale Inhib*., 2019, **8**, no. 3, 549–559. doi: 10.17675/2305-6894-2019-8-3-6
33. M.O. Agafonkina, I.A. Kuznetsov, N.P. Andreeva and Yu.I. Kuznetsov, Copper protection with sodium salts of lower dicarboxylic acids in aqueous neutral solutions, *Int. J. Corros. Scale Inhib*., 2020, **9**, no. 3, 1000–10013. doi: 10.17675/2305-6894-2020-9-3-13
34. Yu.I. Kuznetsov, I.A. Kuznetsov and D.B. Vershok, Protection of copper against corrosion in neutral media by dicarboxylic acid salts, *Int. J. Corros. Scale Inhib*., 2019, **8**, no. 4, 1022–1034. doi: 10.17675/2305-6894-2019-8-4-13
35. D.E. Aspnes, Spectroscopic ellipsometry – Past, present, and future, *Thin Solid Films*, 2014, **571**, 334–344. doi: 10.1016/j.tsf.2014.03.056
36. L. Wang, C. Zhao, M.H.G. Duits, F. Mugele and I. Siretanu, Detection of ion adsorption at solid–liquid interfaces using internal reflection ellipsometry, *Sens. Actuators, B*, 2015, **210**, 649–655. doi: 10.1016/j.snb.2014.12.127
37. R. Longtin, L. Mureşan, M. Porus, P. Maroni, S. Rentsch, M. Buri, P. Gane and M. Borkovec, Probing adsorption of sodium poly(acrylate) at the calcite–water interface by ellipsometry, *Colloids Surf., A*, 2011, **384**, 17–22. doi: 10.1016/j.colsurfa.2011.02.041
38. M. Levin, P. Wiklund and C. Leygraf, Bioorganic compounds as copper corrosion inhibitors in hydrocarbon media, *Corros. Sci*., 2012, **58**, 104–114. doi: 10.1016/j.corsci.2012.01.009

39. W. Ogieglo, H. Wormeester, K-J. Eichhorn, M. Wessling and N.E. Benes, *In situ* ellipsometry studies on swelling of thin polymer films: A review, *Prog. Polym. Sci*., 2015, **42**, 42–78. doi: 10.1016/j.progpolymsci.2014.09.004
40. M.O. Agafonkina, N.P. Andreeva, Yu.I. Kuznetsov and S.F. Timashev, Substituted Benzotriazoles as Inhibitors of Copper Corrosion in Borate Buffer Solutions, *Russ. J. Phys. Chem. A*, 2017, **91**, no. 8, 1414–1421. doi: 10.1134/S0036024417080027
41. F.L. McCrackin, *A Fortran Program for Analysis of Ellipsometer Measurements*, NBS, Technical note 479, 1969.
42. N.P. Andreeva, M.O. Agafonkina and Yu.I. Kuznetsov, *Features of the carboxylates adsorption on copper*, A.N. Frumkin Institute of physical chemistry and electrochemistry. 90th Anniversary. Collection of scientific works, 2019, 246–248 (in Russian).

♦ ♦ ♦